



**Subject Areas:**

42.55.Px, 42.60.Mi,  
05.45.-a, 02.30.Ks

**Keywords:**

semiconductor lasers, cavity solitons,  
delayed feedback, bifurcations, drift  
instability

**Author for correspondence:**

A.G. Vladimirov  
e-mail: [vladimir@wias-berlin.de](mailto:vladimir@wias-berlin.de)

## Cavity solitons in vertical-cavity surface-emitting lasers

A. G. Vladimirov<sup>1,2</sup>, A. Pimenov<sup>1</sup>, S. V.  
Gurevich<sup>3</sup>, K. Panajotov<sup>4,5</sup>, E. Averlant<sup>4,6</sup>,  
and M. Tlidi<sup>6</sup>

Weierstrass Institute, Mohrenstrasse 39, D-10117  
Berlin, Germany <sup>1</sup>

Saint Petersburg State University, Faculty of Physics,  
St. Petersburg, Russia <sup>2</sup>

Institute for Theoretical Physics, University of Münster,  
Wilhelm-Klemm-Str.9, D-48149, Münster, Germany <sup>3</sup>

Department of Applied Physics and Photonics  
(IR-TONA), Vrije Universiteit Brussels, Pleinlaan 2,  
B-1050 Brussels, Belgium <sup>4</sup>

Institute of Solid State Physics, 72 Tzarigradsko  
Chaussee Blvd., 1784 Sofia, Bulgaria <sup>5</sup>

Université Libre de Bruxelles (U.L.B.), Faculté des  
Sciences, CP. 231, Campus Plaine, B-1050 Bruxelles,  
Belgium <sup>6</sup>

We investigate a control of the motion of localized structures of light by means of delay feedback in the transverse section of a broad area nonlinear optical system. The delayed feedback is found to induce a spontaneous motion of a solitary localized structure that is stationary and stable in the absence of feedback. We focus our analysis on an experimentally relevant system namely the Vertical-Cavity Surface-Emitting Laser (VCSEL). We first present an experimental demonstration of the appearance of localized structures in a 80  $\mu\text{m}$  aperture VCSEL. Then, we theoretically investigate the self-mobility properties of the localized structures in the presence of a time-delayed optical feedback and analyze the effect of the feedback phase and the carrier lifetime on the delay-induced spontaneous drift instability of these structures. We show that these two parameters affect strongly the space time dynamics of two-dimensional localized structures. We derive an analytical formula for the threshold associated with drift instability of localized structures and a normal form equation describing the slow time evolution of the speed of the moving structure.

© The Author(s) Published by the Royal Society. All rights reserved.

## 1. Introduction

Transverse localized structures often called cavity solitons were observed experimentally in Vertical-Cavity Surface-Emitting Laser (VCSEL) [1,2]. Due to the maturity of the semiconductor technology and the possible applications of localized structures of light in all-optical delay lines [3] and logic gates [4], these structures have been a subject of an active research in the field of nonlinear optics. Moreover, the fast response time of VCSELs makes them attractive devices for potential applications in all-optical control of light. Localized structures (LSs) appear as solitary peaks or dips on homogeneous background of the field emitted by a nonlinear microresonator with a high Fresnel number. These structures consist of bright or dark pulses in the transverse plane orthogonal to the propagation axis. The spatial confinement of light was investigated since more than two decades (for reviews see [5–10]). When they are sufficiently far away from each other, localized peaks are independent and randomly distributed in space. However, when the distance between the peaks becomes small enough they start to interact via their oscillating, exponentially decaying tails. This interaction then leads to the formation of clusters [11–16]. The relative stability analysis of different LSs of closely packed localized peaks has been carried in [17] near the optical bistability threshold. These stable LSs arise in a dissipative environment and belong to the class of dissipative structures found far from equilibrium. Transport processes like diffraction, dispersion, or diffusion tend to restore spatial uniformity. On the contrary, nonlinearity has a tendency to amplify spatial inhomogeneities. The competition between the transport processes and nonlinearity, leads in dissipative environment to a self-organization phenomenon responsible for the formation of either extended or localized patterns. This is an universal phenomenon that has been theoretically predicted first in the context of reaction-diffusion systems in the seminal papers of Turing, Prigogine, and Lefever [18,19].

Various mechanisms have proven to be responsible for the generation of LSs in VCSELs: coherent optical injection (holding beam, i.e. the part of the optical injection that is used to ensure bistability of the system) in combination with a narrow writing beam (the part of optical injection which is used to perform local switching between the lower branch of the bistability curve and the upper branch) [2,20–22], frequency selective feedback with [23] or without [24] a writing beam, saturable absorption [25], “spatial translational coupling” introduced in [26,27], and others (see [28] for a review).

Localized structures are not necessary stationary objects. They can start to drift spontaneously in the laser transverse section in the presence of saturable absorption [29]. In particular, in the case when the pump beam is axially symmetric LS can move along the boundary on a circular trajectory [30]. It was shown that they can undergo a spontaneous motion due to thermal effects [31,32]. Delayed feedback control is a well documented technique that has been applied to various spatially extended systems in optics, hydrodynamics, chemistry, and biology. It has been demonstrated recently that a simple feedback loop provides a robust and a controllable mechanism is responsible for the motion of LS and localized patterns [33–39]. These works demonstrated that when the product of the delay time and the feedback rate exceeds some threshold value, LS start to move in an arbitrary direction in the transverse section of the device. In these studies, the analysis was restricted to the specific case of nascent optical bistability described by the real Swift-Hohenberg equation with a real feedback term. More recently, analytical study supported by numerical simulations revealed the role of the phase of the delayed feedback and the carrier lifetime on the motion of cavity solitons in a broad-area VCSEL structure, driven by a coherent externally injected beam [39]. It was shown that certain values of the feedback phase LS can be destabilized via a drift bifurcation leading to a spontaneous motion of a solitary two-dimensional LS. Furthermore, the slower is the carrier decay rate in the semiconductor medium, the higher is the threshold associated with the motion of LSs.

The paper is organized as follows. In Sec. 2, we report on an experimental evidence of spontaneous formation of stationary LSs in a 80  $\mu$  m diameter VCSEL biased above the lasing threshold and subjected to optical injection. Such LSs exhibit a bistability when the injected beam

power and the VCSEL current are changed. The static LSs have been found in the absence of delayed feedback. In Sec. 3, we introduce a VCSEL model to study theoretically the effect of time-delayed optical feedback on these structures. In Sec. 4, we investigate the drift instability induced by delayed feedback. We conclude in Sec. 5.

## 2. Experimental observation of stationary LS in medium size VCSELs

In recent years, a considerable amount of experimental work has been realized on stationary localized structures in Vertical-Cavity Surface-Emitting Lasers (VCSELs). They were observed in very broad (aperture  $d > 100\mu\text{m}$ ) [2], broad ( $d \sim 80\mu\text{m}$ ) [40], and medium ( $d \sim 40\mu\text{m}$ ) [41] size VCSELs. Here we present experimental results obtained with bottom-emitting InGaAs multiple quantum well VCSEL with  $d = 80\mu\text{m}$  and threshold current of 42.5 mA at 20°C. The holding (injection) beam is provided by a commercial tunable semiconductor laser (Sacher Lasertechnik TEC100-0960-60 External Cavity Diode Laser), isolated from the rest of the setup by an optical isolator (OFR IO5-TiS2-HP). The long-term electrical and temperature stability of this laser are less than 20 mA RMS and 0.05 °C, respectively. A half-wave plate is used to adjust the linear polarization of the holding beam to be the same as the one of the VCSEL. The injection beam power is tuned using a variable optical density filter. The detuning between the master laser and the VCSEL is defined as  $\theta = \nu_{inj} - \nu_{slave}$ , where  $\nu_{inj}$  is the frequency of the injection beam, and  $\nu_{slave}$  the frequency of the strongest peak in the spectrum of the stand-alone VCSEL. It is experimentally tuned by changing the wavelength of the injection beam. The beam waist  $d_{inj}$  is defined as the diameter of the smallest circle in the plane of propagation of the injection beam containing half of the beam power when it encounters the VCSEL. The power of the source is monitored by a Newport 818-SL photodiode connected to a Newport 2832-C powermeter. The near field is recorded by imaging it on a CCD camera.

An example of stationary LSs is presented in the Fig. 1 illustrating the process of spontaneous creation and annihilation of two-dimensional localized structures. These experimental measurements have been performed when the VCSEL operated in an injection locked regime. The injection beam waist and the detuning are fixed to  $d_{inj} = 50\mu\text{m}$  and  $\theta = -146$  GHz. When increasing the injected beam power, a new LS appears at  $P_{inj} = P_{inj}^{on}$ , as shown in the insets of Fig. 1. This results in a slight jump of the total output power as shown in light-versus-current characteristics. The process of switching-off is realized when decreasing the injection power: the recently created LS persists until  $P_{inj} = P_{inj}^{off}$  with  $P_{inj}^{off} < P_{inj}^{on}$ , i.e. a hysteresis region exists with an additional LS either turned on or off. The two figures on the right show one dimensional scans along the vertical lines indicated in the near field images. Note that the line corresponding to the upper of these two scans intersects a pair of localized structures, as it can be seen from the respective near field image.

Experimental investigation of the effect of the delayed feedback on the mobility properties of the LSs will be a subject of our future work. The delayed optical feedback will be implemented experimentally in a self-imaging external cavity configuration (see e.g. Fig.1 in [33,34]). Using this configuration the effect of diffraction in the external cavity on the feedback field will be minimized, which would allow an implementation of 2D point-to-point optical feedback. As soon as we have provided an experimental evidence of the existence LSs in our 80  $\mu\text{m}$  VCSELs (see Fig. 1), adding such kind of delayed feedback to our experimental setup is a straightforward task. However, in order to detect experimentally the spontaneous drift instability of LSs it is very important to know how the feedback phase and the carrier relaxation rate affect the instability threshold. This problem is addressed theoretically in the next section.

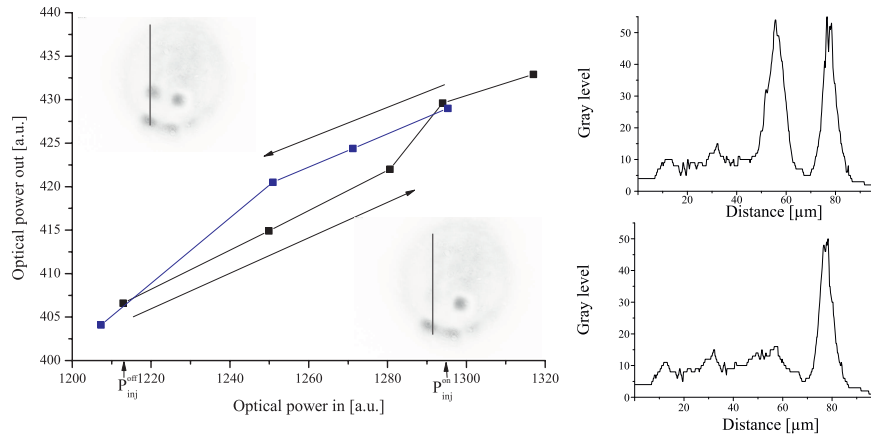


**Figure 1.** Total output power as a function of injection power displaying bistability when a new LS appears. The insets show the near field images of on the upper and the lower branch of the hysteresis curve. The two figures on the right show one dimensional scans along the vertical lines indicated in the near field images.

### 3. Model equations

The mean field model describing the space-time evolution of the electric field envelope  $E$  and the carrier density  $N$  in a VCSEL subjected to optical injection is given by the following set of dimensionless partial differential equations

$$\frac{\partial E}{\partial t} = -(\mu + i\theta)E + 2C(1 - i\alpha)(N - 1)E \quad (3.1)$$

$$+ E_i - \eta e^{i\varphi} E(t - \tau) + i\nabla^2 E,$$

$$\frac{\partial N}{\partial t} = -\gamma \left[ N - I + (N - 1)|E|^2 - d\nabla^2 N \right]. \quad (3.2)$$

Here the parameter  $\alpha$  describes the linewidth enhancement factor,  $\mu$  and  $\theta$  are the cavity decay rate and the cavity detuning parameter, respectively. Below we will assume  $\eta$  to be small enough, so that we can neglect the dependence of the parameters  $\mu$  and  $\theta$  on  $\varphi$ . The parameter  $E_i$  is the amplitude of the injected field,  $C$  is the bistability parameter,  $\gamma$  is the carrier decay rate,  $I$  is the injection current, and  $d$  is the carrier diffusion coefficient. The diffraction of light and the diffusion of the carrier density are described by the terms  $i\nabla^2 E$  and  $d\nabla^2 N$ , respectively, where  $\nabla^2$  is the Laplace operator acting in the transverse plane  $(x, y)$ . Below we consider the case when the laser is subjected to coherent delayed feedback from an external mirror. To minimize the effect of diffraction on the feedback field we assume that the external cavity is self-imaging [33]. The feedback is characterized by the delay time  $\tau = 2L_{ext}/c$ , the feedback rate  $\eta \geq 0$ , and phase  $\varphi$ , where  $L_{ext}$  is the external cavity length, and  $c$  is the speed of light. The link between dimensionless and physical parameters is provided in [34]. Using the expression for the feedback rate  $\eta = \frac{r^{1/2}(1-R)}{R^{1/2}\tau_{in}}$  given in [42], where  $r$  ( $R$ ) is the power reflectivity of the feedback (VCSEL top) mirror and  $\tau_{in}$  is the VCSEL cavity round trip time, we see that the necessary condition for the appearance of the soliton drift instability  $\eta\tau > 1$  [33] can be rewritten in the form  $r > \frac{R\tau_{in}^2}{(1-R)^2\tau^2}$ . In particular, for  $R = 0.3$  and  $\tau = 20\tau_{in}$  the latter inequality becomes  $r > 1.5 \cdot 10^{-3}$ .

### 4. Drift instability threshold

When the delayed feedback is absent,  $\eta = 0$ , Eqs. (3.1) and (3.2) are transformed into the well-known mean field model [43], which supports stable stationary patterns and LSs [2,41,44,45]. It was demonstrated recently that when the feedback rate  $\eta$  exceeds a certain threshold value, which

is inversely proportional to the delay time  $\tau$ , LS starts to move in the transverse direction [33]. Example of moving two-dimensional LS are shown in Fig. 2. The single and the three moving peaks are obtained from numerical simulations of Eqs. (3.1) and (3.2). The boundary conditions are periodic in both transverse dimensions.

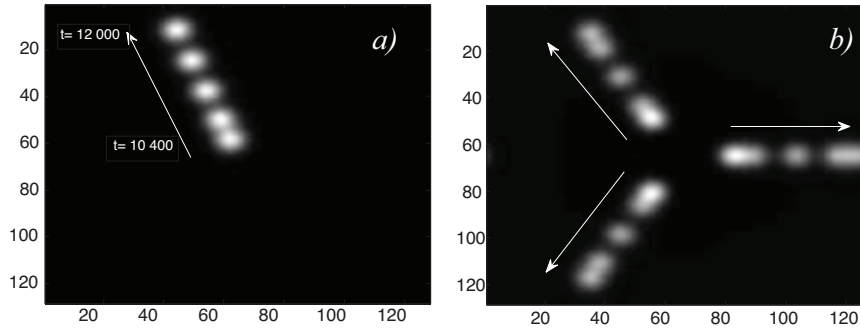


**Figure 2.** Field intensity illustrating a moving single (a) and three (b) peak LS. Parameter values are  $C=0.45$ ,  $\theta = -2$ ,  $\alpha = 5$ ,  $\mu = 1$ , Feedback parameters are  $\eta = 0.135$ ,  $\tau = 100$ ,  $\varphi = 0.5$ . Maxima are plain white.

In the case when the system is transversely isotropic, the velocity of the LS motion has an arbitrary direction. The self-induced motion of the LS is associated with a pitchfork bifurcation where the stationary LS loses stability and a branch of stable LSs uniformly moving with the velocity  $v = |v|$  bifurcates from the stationary LS branch. The bifurcation point can be obtained from the first order expansion of the uniformly moving LS in power series of the small velocity  $v$ . Close to the pitchfork bifurcation point this expansion reads:

$$E(x - vt, y) = E_0(x - vt, y) + vE_1(x - vt, y) + \dots \quad (4.1)$$

$$N(x - vt, y) = N_0(x - vt, y) + vN_1(x - vt, y) + \dots, \quad (4.2)$$

where without the loss of generality we assume that the LS moves along the  $x$ -axis on the  $(x, y)$ -plane. Here  $E_0(x, y) = X_0(x, y) + iY_0(x, y)$  and  $N_0(x, y)$  describes the stationary axially symmetric LS profile, which corresponds to the time-independent solution of Eqs. (3.1) and (3.2) with  $\tau = 0$ . Although formally this solution depends on the feedback parameters  $\eta$  and  $\varphi$  we neglect this dependence assuming that the feedback rate is sufficiently small,  $\eta \ll 1$ . Substituting this expansion into Eqs. (3.1) and (3.2) and collecting the first order terms in small parameter  $v$  we obtain:

$$L \begin{pmatrix} \text{Re } E_1 \\ \text{Im } E_1 \\ N_1 \end{pmatrix} = \begin{pmatrix} \text{Re}[\partial_x E_0(1 - \eta\tau e^{i\varphi})] \\ \text{Im}[\partial_x E_0(1 - \eta\tau e^{i\varphi})] \\ \gamma^{-1} \partial_x N_0 \end{pmatrix} \quad (4.3)$$

where the linear operator  $L$  is given by

$$L = \begin{pmatrix} \mu - 2C(N_0 - 1) & \nabla^2 - \theta - 2C\alpha(N_0 - 1) & -2C(X_0 + \alpha Y_0) \\ -\nabla^2 + \theta + 2C\alpha(N_0 - 1) & \mu - 2C(N_0 - 1) & -2C(Y_0 - \alpha X_0) \\ 2(N_0 - 1)X_0 & 2(N_0 - 1)Y_0 & -d\nabla^2 + 1 + |E_0|^2 \end{pmatrix}.$$

By applying the solvability condition to the right hand side of Eq. (3), we obtain the drift instability threshold

$$\eta\tau = \frac{1 + \gamma^{-1}(b/c)}{\sqrt{1 + (a/c)^2} \cos[\varphi + \arctan(a/c)]} \quad (4.4)$$

with

$$a = \langle \psi_1^\dagger, \psi_2 \rangle - \langle \psi_2^\dagger, \psi_1 \rangle, \quad b = \langle \psi_3^\dagger, \psi_3 \rangle, \quad c = \langle \psi_1^\dagger, \psi_1 \rangle + \langle \psi_2^\dagger, \psi_2 \rangle. \quad (4.5)$$

Here

$$\psi = (\psi_1, \psi_2, \psi_3)^T = \partial_x (X_0, Y_0, N_0)^T \quad (4.6)$$

is a translational neutral mode of the operator  $L$ ,  $L\psi = 0$ , while  $\psi^\dagger = (\psi_1^\dagger, \psi_2^\dagger, \psi_3^\dagger)^T$  is the corresponding solution of the homogeneous adjoint problem  $L^\dagger \psi^\dagger = 0$ . The scalar product  $\langle \cdot \rangle$  is defined as  $\langle \psi_j^\dagger, \psi_k \rangle = \int_{-\infty}^{+\infty} \psi_j^\dagger \psi_k dx dy$ . To estimate the coefficients  $a$  and  $b$  we have calculated the function  $\psi^\dagger$  numerically using the relaxation method in two transverse dimensions,  $(x, y)$ . The results of these calculations are shown in Fig. 3 together with the axially symmetric profile  $E_0$  of the stationary LS. It is seen from this figure that similarly to the neutral mode  $\psi$  defined by (4.6) the neutral mode  $\psi^\dagger$  of the adjoint operator  $L^\dagger$  is an even function of the coordinate  $y$  and an odd function of the coordinate  $x$ , which is parallel to the LS direction of motion.

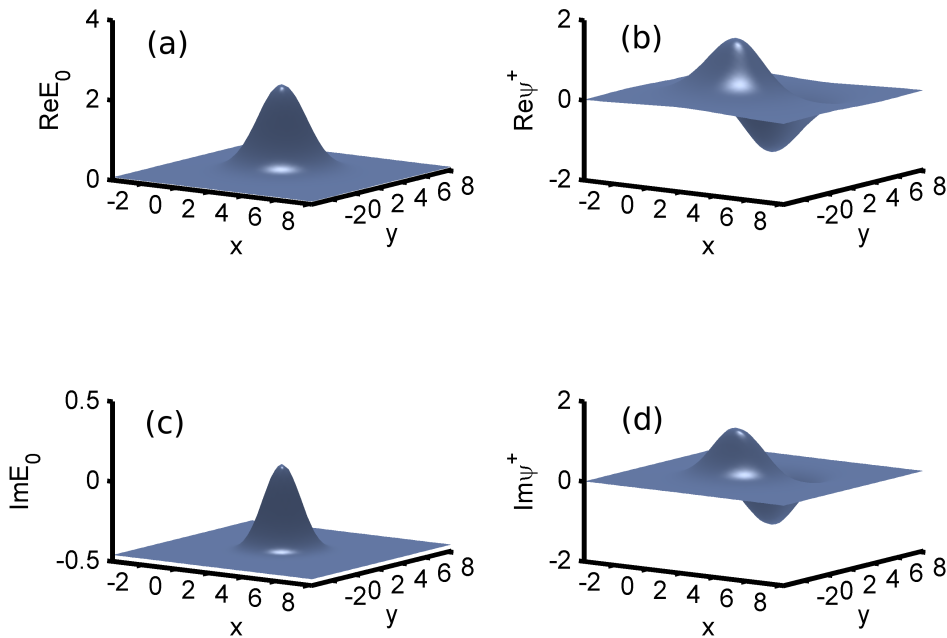


**Figure 3.** Left panels: real and imaginary parts of the stationary soliton profile,  $X_0 = \text{Re } E_0$  (a)  $Y_0 = \text{Im } E_0$  (c). Right panels: real and imaginary parts of the neutral mode of the adjoint operator  $L^\dagger$ ,  $\psi_1^\dagger = \text{Re } \psi^\dagger$  (b) and  $\psi_2^\dagger = \text{Im } \psi^\dagger$  (d). Parameters values:  $\mu = 1.0$ ,  $\theta = -2.0$ ,  $C = 0.45$ ,  $\alpha = 5.0$ ,  $\gamma = 0.05$ ,  $\tau = 100$ ,  $d = 0.052$ ,  $E_i = 0.8$ ,  $I = 2$ .

The dependence of the critical feedback rate  $\eta$  corresponding to the drift instability threshold defined by Eq. (4.4) on the feedback phase  $\varphi$  and carrier relaxation rate  $\gamma$  is illustrated by Fig. 4. In this figure the curves labeled by different numbers correspond to different values of  $\gamma$ . Considering the fact that the feedback in Eq. (3.1) is introduced with the minus sign, we see that the drift instability takes place only for those feedback phases when the interference between the cavity field and the feedback field is destructive, i.e. when  $\cos$  function in the denominator of the right hand side of Eq. (4.4) is positive. On the contrary, when this interference is constructive the feedback has a stabilizing effect on the LS. Furthermore, the slower is the carrier relaxation rate, the higher is the drift instability threshold. Since the stationary LS solution does not depend on the carrier relaxation rate  $\gamma$ , the coefficients  $a$  and  $b$  in the threshold condition (4.4) are also independent of  $\gamma$ . Therefore, (4.4) gives an explicit dependence of the threshold feedback rate on

the carrier relaxation rate. In particular, in the limit of very fast carrier response,  $\gamma \gg 1$ , and zero feedback phase,  $\varphi = 0$ , we recover from (4.4) the threshold condition  $\eta\tau = 1$  which was obtained earlier for the LS drift instability induced by a delayed feedback in the real Swift-Hohenberg equation [33]. Note that at  $\gamma \rightarrow \infty$ ,  $a \neq 0$ , and  $\varphi = -\arctan a$  the critical feedback rate appears to be smaller than that obtained for the real Swift-Hohenberg equation,  $\eta\tau = (1 + a^2)^{-1/2} < 1$ .

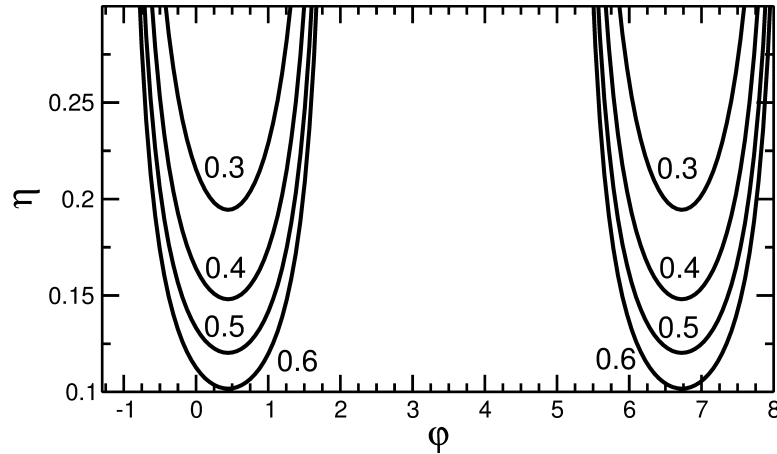


**Figure 4.** Critical value of the feedback rate  $\eta$  corresponding to the drift bifurcation vs feedback phase  $\varphi$  calculated for different values of the carrier relaxation rate  $\gamma$ . The values of the parameter  $\gamma$  are shown in the figure. Other parameters are the same as in Fig. 3.

As it was demonstrated above, the bifurcation threshold responsible for self-induced drift of LS in the VCSEL transverse section is obtained by expanding the slowly moving localized solution in the small velocity  $v$ , substituting this expansion into the model equations (3.1),(3.2), and matching the first order terms in  $v$ . In order to describe the slow evolution of the LS velocity slightly above the bifurcation threshold, one needs to perform a similar procedure with  $E = E_0(x - x_0(t), y) + \sum_{k=1}^3 \epsilon^k E_k(x - x_0(t), y, t) + \dots$  and  $N = N_0(x - x_0(t), y) + \sum_{k=1}^3 \epsilon^k N_k(x - x_0(t), y, t) + \dots$ , where  $dx/dt = v(t) = \mathcal{O}(\epsilon)$ ,  $dv/dt = \mathcal{O}(\epsilon^3)$  and  $\epsilon$  is a small parameter characterizing the distance from the bifurcation point. Then, omitting detailed calculations, in the third order in  $\epsilon$ , we obtain the normal form equation for the LS velocity:

$$\frac{p}{2} \frac{dv}{dt} = v(\delta\eta q - \eta\tau^2 r v^2), \quad (4.7)$$

where  $\delta\eta$  is the deviation of the feedback rate from the bifurcation point. The coefficients  $q$ ,  $p$ , and  $r$  are given by  $q = a \sin \varphi + c \cos \varphi$ ,  $p = q + b$ , and  $r = f \sin \varphi + g \cos \varphi + \mathcal{O}(\tau^{-1})$ , respectively. Here  $a$ ,  $b$ , and  $c$  are defined by Eq. (4.5) and  $f = \langle \psi_1^\dagger, \partial_{xxx} Y_0 \rangle - \langle \psi_2^\dagger, \partial_{xxx} X_0 \rangle$ ,  $h = \langle \psi_3^\dagger, \partial_{xxx} N_0 \rangle$ ,  $g = \langle \psi_1^\dagger, \partial_{xxx} X_0 \rangle + \langle \psi_2^\dagger, \partial_{xxx} Y_0 \rangle$ . The stationary LS velocity above the drift instability threshold is obtained by calculating the nontrivial steady state of Eq. (4.7),  $v = \sqrt{\delta\eta} Q$ , where the coefficient  $Q = (1/\tau) \sqrt{q/(r\eta)}$  determines how fast the LS velocity increases with the square root of the deviation from the critical feedback rate. The dependence of this coefficient on the feedback phase is illustrated by Fig. 5.

## 5. Conclusion

In the first part of the paper we have investigated experimentally the formation of transverse LSs of light in a medium size bottom-emitting InGaAs multiple quantum well VCSEL operated in an injection locked regime. Creation and annihilation of a single LS have been demonstrated by

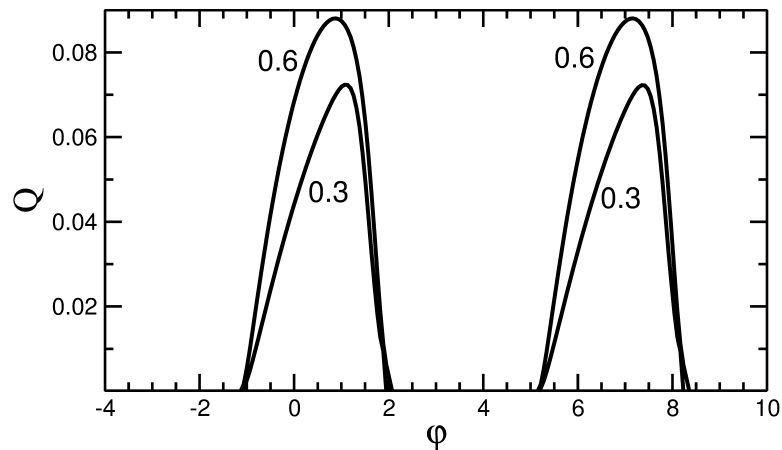


**Figure 5.** Coefficient  $Q$  describing the growth rate of the LS velocity with the square root of the deviation from the critical feedback rate. The values of the parameter  $\gamma$  are shown in the figure. Other parameters are the same as in Fig. 3.

changing the injection beam power. In the experimental part the localized peaks were stationary since delayed feedback was not applied to the laser.

In the second part, we have analyzed theoretically the effect of time delayed feedback from an external mirror on the stability of transverse localized structures in a broad area VCSEL. We have shown that depending on the phase of the feedback it can have either destabilizing or stabilizing effect on the LSs. In particular, when the interference between the LS field and the feedback field is destructive, the LS can be destabilized via a pitchfork bifurcation, where a branch of uniformly moving LS bifurcates from the stationary one. We have calculated analytically the threshold value of the feedback rate corresponding to this bifurcation and demonstrated that the faster is the carrier relaxation rate in the semiconductor medium, the lower is the threshold of the spontaneous drift instability induced by the feedback. Finally, we have derived the normal form for equation (4.7) governing the slow dynamics of the LS velocity. This generic destabilization mechanism is robust in one and two spatial dimensions and could be applied to a large class of far from equilibrium systems under time-delay control.

Our future work will be focused on the experimental investigation of the effect delayed feedback on the spontaneous motion of LSs. This study would allow us to check the theoretical predictions of Sec. 4. We are also planning to investigate the role of local polarization dynamics in the formation of LSs in the transverse plane of the VCSEL. This would allow us to study the spontaneous motion of vector LSs with different polarizations, which is induced by delayed feedback.

## Acknowledgment

A.G.V. and A.P. acknowledge the support from SFB 787 of the DFG. A.G.V. acknowledges the support of the EU FP7 ITN PROPHET and E.T.S. Walton Visitors Award of the Science Foundation Ireland. M.T. received support from the Fonds National de la Recherche Scientifique (Belgium). This research was supported in part by the Interuniversity Attraction Poles program of the Belgian Science Policy Office under Grant No. IAP P7-35.

## References

1. V. B. Taranenko, I. Ganne, R. J. Kuszelewicz, and C. O. Weiss, *Patterns and localized structures in bistable semiconductor resonators*, Phys. Rev. A **61**, 063818 (2000).



2. S. Barland, J. R. Tredicce, M. Brambilla, L. A. Lugiato, S. Balle, M. Giudici, T. Maggipinto, L. Spinelli, G. Tissoni, T. Knodl, *Cavity solitons as pixels in semiconductor microcavities*, Nature **419**, 699 (2002).
3. F. Pedaci, S. Barland, E. Caboche, P. Genevet, M. Giudici, J. R. Tredicce, T. Ackemann, A. J. Scroggie, W. J. Firth, G. L. Oppo, G. Tissoni, and R. Jager, *All-optical delay line using semiconductor cavity solitons*, Appl. Phys. Lett. **92**, 011101 (2008).
4. A. Jacobo, D. Gomila, M. A. Matías, and P. Colet, *Logical operations with localized structures*, New J. Phys. **14**, 013040 (2012).
5. L.A. Lugiato, *Transverse nonlinear optics: Introduction and review*, Chaos, Solitons and Fractals, **4**, 1251 (1994)
6. N.N. Rosanov, *Transverse Patterns in Wide-Aperture Nonlinear Optical Systems*, Progress in Optics, **35**, 1 (1996)
7. K. Staliunas and V.J. Sanchez-Morcillo, *Transverse Patterns in Nonlinear Optical Resonators*, (Springer Tracts in Modern Physics (Springer-Verlag, Berlin Heidelberg, 2003)
8. Y.S. Kivshar and G.P. Agrawal, *Optical Solitons: from Fiber to Photonic Crystals* (Amsterdam, Academic press, Elsevier Science (2003)
9. P. F. Mandel and M. Tlidi, *Transverse dynamics in cavity nonlinear optics (2000-2003)*, J. Opt. B: Quant. Semiclass. Opt. **6**, R60 (2004).
10. T. Ackemann, W.J. Firth, G.L.Oppo, *Advances in Atomic Molecular and Optical Physics*, **57**, 323 (2009).
11. A. G. Vladimirov, G. V. Khodova, and N. N. Rosanov, *Stable bound states of one-dimensional autosolitons in a bistable laser*, Phys. Rev. E **63**, 056607 (2001).
12. A. G. Vladimirov, J. M. McSloy, D. V. Skryabin, and W. J. Firth, *Two-dimensional clusters of solitary structures in driven optical cavities*, Phys. Rev. E **65**, 046606 (2002).
13. M. Tlidi, A. G. Vladimirov, P. Mandel, *Interaction and stability of periodic and localized structures in optical bistable systems*, IEEE J. Quant. Electron. **39**, 216 (2003).
14. D. Turaev, A. G. Vladimirov, and S. Zelik, *Chaotic bound state of localized structures in the complex Ginzburg-Landau equation*, Phys. Rev. E **75**, 045601 (2007).
15. D. Turaev, A. G. Vladimirov, and S. Zelik, *Long-Range Interaction and Synchronization of Oscillating Dissipative Solitons* Phys. Rev. Lett. **108**, 263906 (2012).
16. M. Tlidi, R. Lefever, and A. G. Vladimirov, *On vegetation clustering, localized bare soil spots and fairy circles*, in *Dissipative solitons: From optics to biology and medicine* (Lecture Notes in Physics, Vol. 751) Akhmediev, Nail; Ankiewicz, Adrian (Eds.) (2008)
17. A. G. Vladimirov, M. Tlidi, and R. Lefever, *Relative stability of multipeak localized patterns of cavity solitons*, Phys. Rev. A **84**, 043848 (2011).
18. A. Turing, *The chemical basis of morphogenesis*, Phil. Trans. R. Soc. London **237**, 37 (1952).
19. I. Prigogine and R. Lefever, *Symmetry breaking instabilities in dissipative systems. II*, J. Chem. Phys. **48**, 1695 (1968).
20. Y. Menesguen, S. Barbay, X. Hachair, L. Leroy, I. Sagnes, and R. Kuszelewicz, *Optical self-organization and cavity solitons in optically pumped semiconductor microresonators*, Phys. Rev. A **74**, 023818 (2006).
21. Y. Larionova and C. O. Weiss, *Spatial semiconductor resonator solitons with optical pumping*, Opt. Express **13**, 10711 (2005).
22. X. Hachair, F. Pedaci, E. Caboche, S. Barland, M. Giudici, J. R. Tredicce, F. Prati, G. Tissoni, R. Kheradmand, L. A. Lugiato, I. Protsenko, and M. Brambilla, *Cavity solitons in a driven vcsel above threshold*, IEEE J. Sel. Top. Quantum Electron. **12**, 339 (2006).
23. Y. Tanguy, T. Ackemann, W. J. Firth, and R. Jager, *Realization of a semiconductor-based cavity soliton laser*, Phys. Rev. Lett. **100**, 013907 (2008).
24. N. Radwell and T. Ackemann, *Characteristics of laser cavity solitons in a vertical-cavity surface-emitting laser with feedback from a volume bragg grating*, IEEE J. Quantum Electron. **45**, 1388 (2009).
25. P. Genevet, S. Barland, M. Giudici, and J. R. Tredicce, *Cavity soliton laser based on mutually coupled semiconductor microresonators*, Phys. Rev. Lett. **101**, 123905 (2008).
26. A. F. Haudin, R. G. Rojas, U. Bortolozzo, M. G. Clerc, and S. Residori, *Vortex emission accompanies the advection of optical localized structures*, Phys. Rev. Lett. **106**, 063901 (2011).
27. F. del Campo, F. Haudin, R. G. Rojas, U. Bortolozzo, M. G. Clerc, and S. Residori, *Effects of translational coupling on dissipative localized states*, Phys. Rev. E **86**, 036201 (2012).
28. S. Barbay, R. Kuszelewicz, and J. R. Tredicce, *Cavity solitons in vcsel devices*, Adv. Opt. Technol. **2011**, 628761 (2011)

29. S. V. Fedorov, A. G. Vladimirov, G. V. Khodova, and N. N. Rosanov, *Effect of frequency detunings and finite relaxation rates on laser localized structures*, Phys. Rev. E 61, 5814 (2000).
30. F. Prati, G. Tissoni, L. A. Lugiato, K. M. Aghdami, and M. Brambilla, *Spontaneously moving solitons in a cavity soliton laser with circular section*, Eur. Phys. J. D 59, 73-79 (2010).
31. L. Spinelli, G. Tissoni, L. A. Lugiato, and M. Brambilla, *Thermal effects and transverse structures in semiconductor microcavities with population inversion*, Phys. Rev. A 66, 023817 (2002).
32. A. J. Scroggie, J. M. McSloy, and W. J. Firth, *Self-propelled cavity solitons in semiconductor microcavities*, Phys. Rev. E 66, 036607 (2002).
33. M. Tlidi, A. G. Vladimirov, D. Pieroux, and D. Turaev, *Spontaneous motion of cavity solitons induced by a delayed feedback*, Phys. Rev. Lett. 103, 103904 (2009).
34. K. Panajotov and M. Tlidi, *Spontaneous motion of cavity solitons in vertical-cavity lasers subject to optical injection and to delayed feedback*, Eur. Phys. J. D 59, 67 (2010).
35. M. Tlidi, E. Averlant, A. Vladimirov, and K. Panajotov, *Delay feedback induces a spontaneous motion of two-dimensional cavity solitons in driven semiconductor microcavities*, Phys. Rev. A 86, 033822 (2012).
36. S. V. Gurevich and R. Friedrich, *Instabilities of localized structures in dissipative systems with delayed feed-back*, Phys. Rev. Lett. 110, 014101 (2013).
37. M. Tlidi, A. Sonnino, and G. Sonnino, *Delayed feedback induces motion of localized spots in reaction-diffusion systems*, Phys. Rev. E 87, 042918 (2013).
38. S. V. Gurevich, *Dynamics of localized structures in reaction-diffusion systems induced by delayed feedback*, Phys. Rev. E 87, 052922 (2013).
39. A. Pimenov, A. G. Vladimirov, S. V. Gurevich, K. Panajotov, G. Huyet, and M. Tlidi, *Delayed feedback control of self-mobile cavity solitons*, Phys. Rev. A 88, 053830 (2013).
40. E. Averlant, M. Tlidi, H. Thienpont, T. Ackemann, and K. Panajotov, *Experimental observation of localized structures in medium size VCSELs*, Opt. Express 22, 762 (2014).
41. X. Hachair, G. Tissoni, H. Thienpont, and K. Panajotov, *Linearly polarized bistable localized structure in medium-size vertical-cavity surface-emitting lasers*, Phys. Rev. A 79, 011801 (2009).
42. G. H. M. van Tartwijk and D. Lenstra, *Semiconductor lasers with optical injection and feedback*, J. Opt. B Quantum Semiclassical Opt. 7, 87-144 (1995).
43. L. Spinelli, G. Tissoni, M. Brambilla, F. Prati, and L. A. Lugiato, *Spatial solitons in semiconductor microcavities*, Phys. Rev. A 79, 2542 (1998).
44. X. Hachair, S. Barland, L. Furfaro, M. Giudici, S. Balle, J.R. Tredicce, M. Brambilla, T. Maggipinto, I.M. Perrini, G. Tissoni, and L. Lugiato, *Cavity solitons in broad-area vertical-cavity surface-emitting lasers below threshold*, Phys. Rev. A 69, 043817 (2004).
45. X. Hachair, L. Furfaro, J. Javaloyes, M. Giudici, S. Balle, J. Tredicce, G. Tissoni, L.A. Lugiato, M. Brambilla, and T. Maggipinto, *Cavity-solitons switching in semiconductor microcavities*, Phys. Rev. A 72, 013815 (2005).